*Proceedings of the 21st ICSMGE, Vienna, Austria, 14 – 19 June 2026. Pistrol, Adam & Schweiger (eds.)*
*Published by: ÖGG, Austrian Society for Geomechanics, Salzburg, Austria, ISBN 978-3-9503898-4-5*
*https://doi.org/10.53243/ICSMGE2026-306*

# 3D Numerical Modelling of Thermal Performance and Optimisation of Thermo-Active Roads

**Junjia Lyu,** Nikolas Makasis, Liang Cui, Benyi Cao
*School of Engineering, University of Surrey, Guildford, UK, j.lyu@surrey.ac.uk*

ABSTRACT: Thermo-active roads are a relatively new type of energy geostructures, which involves two sets of horizontally placed pipes at different depths to exchange heat between the pavement surface and the ground. Thereby, thermal energy can be stored into the ground beneath the road in summer and can be extracted and used to heat up the road surface in winter. This research developed a detailed three-dimensional (3D) finite-element (FE) model in COMSOL Multiphysics to explore the thermal performance of a thermo-active road. The 3D FE model developed was extensively validated against a field test data and then the system was optimised with key design parameters to raise energy harvesting and extracting efficiency of the geothermal system. Results indicate that the energy storage and release efficiencies can be increased by factors of 3.01 and 1.60, respectively, when an insulation layer is applied, and by factors of 3.51 and 1.46, respectively, when no insulation layer is used.

KEYWORDS: Thermo-active road; Thermal performance; Temperature regulation.

## 1 INTRODUCTION

Roads are vital infrastructure, facilitating economic growth and enabling connectivity within communities. However, freeze-thaw cycles present significant challenges to road infrastructure, undermining the structural integrity of pavements. These cycles accelerate the deterioration of road surfaces, leading to widespread cracking, potholes, and a reduced lifespan of pavements (Si et al.2014). This degradation not only increases the cost of road maintenance and vehicle repairs but also contributes to higher greenhouse gas (GHG) emissions, exacerbating environmental concerns (Ogwang 2019). Therefore, the development of innovative solutions to mitigate these impacts is essential to ensure the longevity and efficiency of transportation networks.

One promising approach to addressing these issues is to use thermo-active roads (Gu et al. 2022), which regulate pavement surface temperatures to reduce damage caused by freeze-thaw cycles and other seasonal fluctuations. Thermo-active roads are designed to control pavement temperatures through the incorporation of energy systems such as ground source heat pumps (GSHP) or self-heating loops, potentially reducing the impact of rutting in the summer and cracking in the winter. While several studies have explored the use of such systems for purposes like snow melting (Zhao et al.2020) and surface de-icing (Bowers et al. 2014), there is a gap in understanding the broader application of these technologies for temperature regulation throughout the year.

This research develops a validated numerical model for a thermo-active road aiming at investigating the system heat harvesting and pavement temperature regulation. The detailed 3D FE numerical model is applied to simulate the thermal performance of the thermo-active road in a field test in Toddington, UK (Carder et al. 2007), incorporating the governing equations of boundaries and interfaces. The temperature change at different layers has been plotted to analyse the performance of the system. The energy storage and release in different seasons are calculated with the varying fluid temperature. After the validation, key parameters are considered as variables to optimise the thermal performance of the system (Hou et al. 2022; Pu et al. 2018). This study focuses on revealing the feasibility to store thermal energy into the ground beneath the thermo-active road in summer for heating up the road surface in winter. On this basis, this study also shows that this system can regulate road temperature, thereby reducing surface damage and extending its lifespan.

## 2 METHODOLOGY

### 2.1 *Governing Equations for Multiphysics Processes*

The modelling of the thermo-active road was implemented in the FE package, COMSOL Multiphysics (COMSOL 6.2, 2024). The governing equations for fluid flow and heat transfer are numerically coupled to capture the heat transfer between the circulating fluid in the pipes and surrounding ground.

Fourier's Law governs the principle of heat transfer between soil and pavement layers, which can be written as:

$$\rho C_p \frac{\partial T}{\partial t} + \rho C_p \mathrm{u} \cdot \nabla T - \nabla \cdot (k \nabla T) = Q + Q_{ted} \quad (1)$$

where u is the fluid velocity; $\rho$, $k$ and $C_p$ are the density, thermal conductivity and specific heat capacity respectively; $T$ represents the temperature, while $Q$ represents the heat source; $Q_{ted}$ is thermoelastic damping.

The momentum and continuity equations for flow in a pipe are given by Barnard et al. (1966):

$$\rho \frac{\partial u}{\partial t} + \rho u \cdot \nabla u = -\nabla p - f_D \frac{\rho}{2 d_h} u|u| + F \quad (2)$$

$$\frac{\partial A\rho}{\partial t} + \nabla \cdot (\mathrm{A}\rho u) = 0 \quad (3)$$

where $u$ is the fluid velocity while $p$ is the fluid pressure, and $\rho$ is the density of the fluid; $f_D$, A, and $d_h$ represent the Darcy friction factor, the cross-section area and mean hydraulic diameter of the pipe respectively, and $F$ is a volume force term.

As for the governing equation for heat transfer within the fluid, it can be written as:

$$\rho A C_p \frac{\partial T}{\partial t} + \rho A C_p u \cdot \nabla T = \nabla \cdot (Ak \nabla T) + \frac{1}{2} f_D \frac{\rho A}{2 d_h} |u| u^2 + Q + Q_{wall} \quad (4)$$

where $Q_{wall}$ represents the heat exchange through the pipe wall.

The heat transfer in soil, pavement layers and pipe flow, is coupled through the temperature field, for the latter using $Q_{wall}$ to link the fluid temperature inside the pipes to the soil temperature at the external pipe wall.

### 2.2 *Model Development*

The configuration comprises two sets of pipe arrays that work as ground heat exchangers (GHEs). Both collector and storage pipe arrays are comprised of 10 pipes with a length of 30 m along the direction of the road and 5 m in width both. In this study, the pipe arrays are referred to as either collector pipes or storage pipes according to their depth. The 3D illustration of the system is shown in Figure 1. Collector pipes are those installed

at 0.12 m depth directly below the road surface while storage pipes are those installed at a depth of 0.86 m. The fluid used as a heat carrier is water. The circulating fluid flows from collector pipes to storage pipes, while the fluid outflowing from storage pipes will be pumped back to the inlets of collector pipes. The pipes themselves are made of cross-linked polyethylene with a diameter of 0.025 m and a spacing of 0.25 m between adjacent longitudinal runs. A 0.2 m thick polystyrene insulation layer is placed on top of the storage pipes to minimise heat losses to the soil surface. As the heat pump brings a larger cost in both installation and operation processes, this research considers the use of an ordinary water pump instead of a heat pump if the energy harvesting efficiency is sufficient. The material properties of different layers are shown in Table 1, and the parameters of pipes are shown in Table 2.

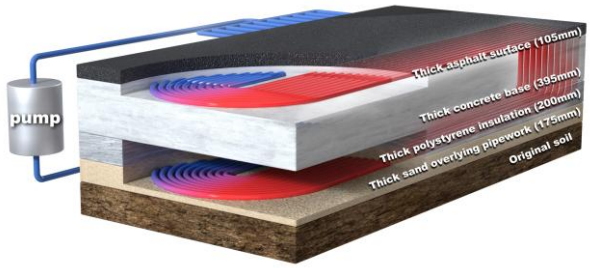


Figure 1. 3D sketch of the system.

Table 1. Material parameters used for numerical analysis.

| Material Type | Density (kg/m³) | Specific Heat (J/kg·K) | Thermal Conductivity (W/m·K) |
|---|---|---|---|
| Asphalt | 2400 | 850 | 0.85 |
| Concrete | 2100 | 840 | 1.4 |
| Polystyrene | 30 | 1130 | 0.034 |
| Sand | 2240 | 840 | 0.33 |
| Soil | 1960 | 1127 | 1.21 |

Table 2. Pipe system data used for numerical analysis.

| Parameters | Values |
|---|---|
| Pipe diameter (m) | 0.025 |
| Thickness of pipe wall (m) | 0.0023 |
| Length of pipes (straight section) (m) | 60 |
| Number of pipes per heat exchanger | 10 |
| Pipe thermal conductivity (W/m·K) | 0.4 |
| Flow rate* (L/s) | 1.4 |

*Total flow rate was 1.4 L/s between the collector and storage pipe arrays, i.e. 0.14L/s through each of the ten flow and return pipes.

The initial temperature of both the ground and the far-field boundaries are equal to the measured undisturbed ground temperature $T$ for different depths $z$, that is, $T_{ground}(z)$, which can be seen in Figure 2. The initial fluid temperature is set as 11 ˚C. The boundary condition of far-field side and bottom boundaries are set as thermal insulation which renders a zero net flux at the interface. While fully insulated far-field boundary conditions are commonly employed, they may slightly underestimate long-term heat dissipation to the surrounding soil, potentially leading to a modest overestimation of storage performance. However, for a one-year operation period, this influence is expected to be minimal. To minimise the effects of solar radiation, shading and wind speed, this research directly using the pavement surface temperature measured during field test as a boundary condition applied to the pavement surface.

The fluid flow within the pipes is assumed to be fully developed which means it does not change along the direction of flow. The inlet and outlet fluid temperature of storage pipes can be measured in the model. The energy transferred into or out of the surrounded soil can be determined through a function of the inlet and outlet fluid temperature (Selamat et al. 2016):

$$Q(t) = C_{p,w}\dot{m}\left(T_{in}(t) - T_{out}(t)\right) \quad (5)$$

where $Q$ is the energy transferred between fluid and soil, $\dot{m}$ is the mass flow rate (kg/s), $C_{p,w}$ is the specific heat capacity of the fluid (J/(kg·K)).

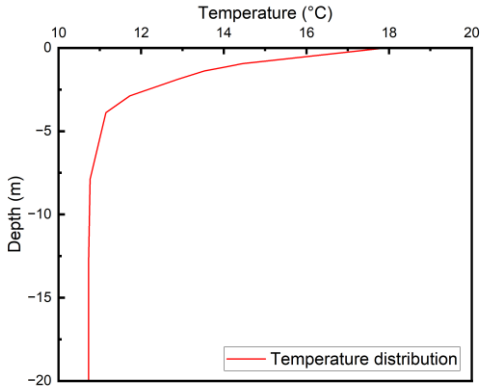


Figure 2. Initial ground temperature distribution along depth.

### 2.3 *Thermal Performance Assessment*

To simulate and evaluate the thermal performance of the system, the whole operation process is divided into three periods, energy storage period, seasonal transition period, and energy release period.

The energy storage period takes 42 days. The pump turns on to circulate the fluid to carry the heat absorbed at the surface into the storage region. In the first 20 days, the fluid in the heat exchangers is pumped when the temperature difference between the temperature sensor located at the middle of the collector pipes and that located at the middle of the storage pipes is larger than 4 ˚C, representing the situation where available heat/coolth can be transferred to/from the storage pipes. Once active, the pumps are turned off when the temperature difference drops below 3.5 ˚C. As the process of energy storage develops, the temperature in collector level and storage level is converging each other, resulting in the permanent deactivation of the pump. To raise the efficiency of the system, after 20 days, the pump is turned on when the temperature difference is larger than 1.5 ˚C, and once active, it is turned off when the temperature difference drops below 1 ˚C.

The seasonal transition period takes 42 days, and in this period the operation of the system is paused. The soil in the storage region is prevented from being heated normally due to the presence of the insulation layer. The energy release period takes 97 days. The pumps are activated when the temperature of the pavement surface falls below 5 ˚C and turned off when the pavement surface temperature increases above 5 ˚C.

## 3 NUMERICAL MODEL VALIDATION

The red region in Figure 3 illustrates the pavement surface temperature during the energy storage process in summer, with a maximum temperature of 39.96 °C and a minimum of 8.59 °C. The seasonal transition period is represented by the yellow region. During the energy release period, depicted in blue, temperatures range from a maximum of 13.71 °C to a minimum of -3.00 °C.

### 3.1 *Energy Storage Period*

The temperature variations at depths of -0.01 m, -0.12 m, and -0.86 m throughout the entire period is presented in Figure 4. The black line representing surface temperature shows the greatest fluctuations, while the ground temperature at the collector pipe level exhibits less variation. The ground temperature at the storage pipe level remains relatively stable due to the insulation layer separating the collector and storage pipes. The overall upward trend indicates thermal energy storage in the soil.

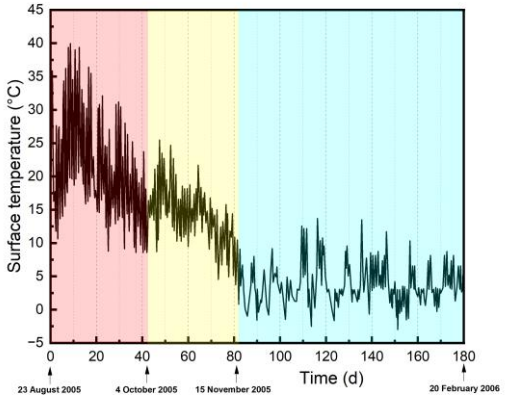


Figure 3. Road surface temperature from 23 August, 2005 to 20 February, 2006.

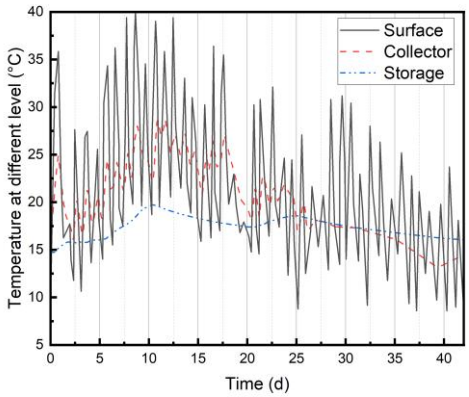


Figure 4. Ground temperature at different depths.

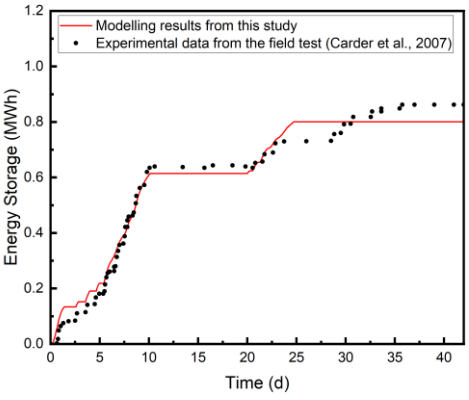


Figure 5. Accumulative energy storage during energy storage period.

In terms of the validation results, the simulation predicts a total energy storage of 0.80 MWh, while the reported experimental value is 0.86 MWh, resulting in a relative error of 6.98% (Figure 5).

The temperature variation for different depths both in numerical and experimental results is shown in Figure 6. For deeper soil temperatures (1.88-12.88 m) from the modelling results align very well, with a maximum error of 1.32%. The discrepancies for shallower soil temperatures (0.88-1.38 m) are relatively larger, with a maximum error of 6.80%. Overall, the model aligns well with in-situ experimental data, facilitating analysis of the contour temperature profile near the road surface at the end of the energy storage period.

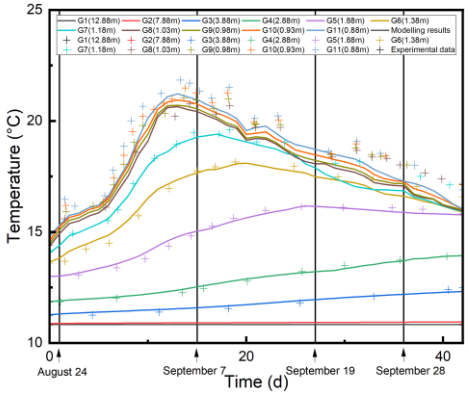


Figure 6. Comparisons of temperature variation for each depth between modelling results and experimental data.

### 3.2 *Seasonal Transition Period*

During this period, the water in the pipes is not circulating and both the soil near the surface and the pipes is cooling gradually. There is no heat collection or usage occurred beneath the insulation layer, except the heat dissipation.

### 3.3 *Energy Release Period*

The ground temperature at the collector pipe level changes much less than the surface temperature. The minimum temperature at collector level is 1.13 °C at the 45$^{th}$ hour, indicating that the system has the potential to regulate the pavement temperature above freezing point, thereby protecting the road from cracking by reducing freeze-thaw cycles. The downward trend of storage level temperature indicates that thermal energy is being released to warm the upper soil.

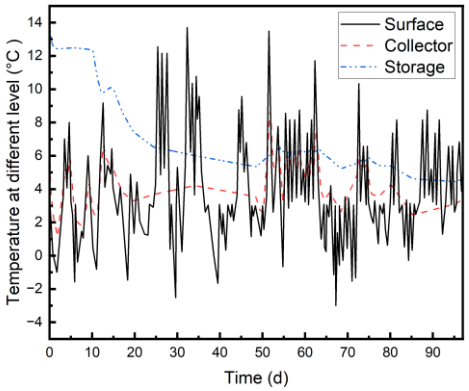


Figure 7. Ground temperature at different depths.

The total simulated energy release is 2.82 MWh, while the experimental value is 2.86 MWh, resulting in a relative error of 1.40% (Figure 8).

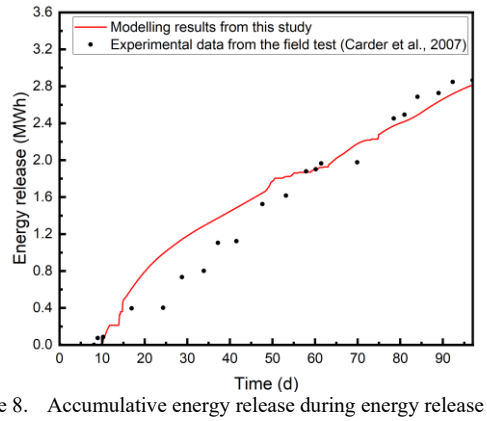


Figure 8. Accumulative energy release during energy release period.

The energy storage efficiency is 19.05 kWh/d, while the energy release efficiency is 29.07 kWh/d. This suggests that some optimisation is needed to improve energy storage efficiency.

## 4 SYSTEM OPTIMISATION

The optimisation was conducted using a parametric sweep approach, in which soil thermal conductivity, pipe depth and flow rate were systematically varied within predefined feasible ranges to identify the parameter combinations that maximise the storage and release efficiencies. The optimised parameter values are listed in Table 3. A sensitivity analysis was conducted to evaluate the selected parameters. Storage/release efficiencies were most sensitive to the embedded depth of the storage pipes, with a 1.54 m increase resulting in 1.75/1.44 times higher values. Increasing soil thermal conductivity improved the energy release by 16%. Both parameters remain within ranges reported in the literature, providing guidance for system design and optimisation. With the inclusion of an insulation layer, the accumulative energy storage reaches 2.41 MWh, compared to 2.14 MWh without insulation layer (Figure 9a), corresponding to 12.62% higher storage efficiency. The energy storage efficiency improves by factors of 3.01 and 3.51, respectively. In terms of the energy release period, the accumulative energy release is 4.52 MWh with insulation layer, compared to 3.68 MWh without insulation layer (Figure 9b), a 22.83% improvement, indicating that the insulation layer effectively mitigates energy leakage. The energy release efficiency is enhanced by factors of 1.60 and 1.46, respectively.

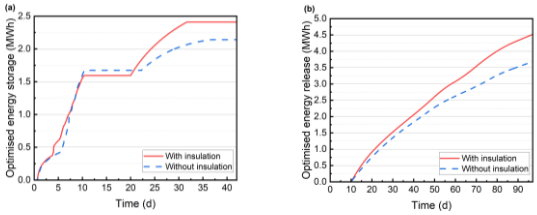


Figure 9. (a) Optimised accumulative energy storage with/without insulation layer. (b) Optimised accumulative energy release with/without insulation layer.

Table 3. Value selections of key parameters in design optimisation.

| Parameters | Values |
|---|---|
| Soil thermal conductivity | 2.0 W/(m·K) |
| Depth of collector pipes | 0.08 m |
| Depth of storage pipes | 2.4 m |
| Flow rate | 2.2 L/s |

It is shown that the parametric optimisation has a larger impact on energy storage period than on energy release period. The energy storage efficiency of the system with insulation layer is 57.38 kWh/d, while the energy release efficiency is 46.60 kWh/d. Therefore, the system can achieve self-sufficiency after optimisation.

## 5 CONCLUSIONS

This research has investigated the thermal performance of a thermo-active road during a full cycle of energy harvesting and releasing. The key findings are summarised below:

1. A developed FE modelling methodology has been validated with a maximum relative error of 6.98% for energy storage value and 1.40% for energy release value.
2. The thermo-active roads have the potential to reduce the number of freeze-thaw cycles and protect the road from cracking in winter as well.
3. After parametric optimisation, the energy storage efficiency increases to 57.38 kWh/d, while the energy release efficiency reaches 46.60 kWh/d, thereby achieving self-sufficiency.
4. With the optimisation of all parameters, the energy storage and release efficiency of the system can be enhanced by factors of 3.01 and 1.60 respectively with insulation layer, while by factors of 3.51 and 1.46 respectively without insulation layer.

## 6 ACKNOWLEDGEMENTS

This work was supported by the Royal Academy of Engineering (RF2223-22-118), the Royal Society (RG\R2\232260), and an Energy Systems Cluster studentship from University of Surrey.

## 7 REFERENCES

A. C. L. Barnard, W. A. Hunt, W. P. Timlake, and E. Varley 1966. A Theory of Fluid Flow in Compliant Tubes. Biophysics Journal, 6, 717-724.

Allan Ogwang, Samer Madanat, Arpad Horvath 2019. Optimal Cracking Threshold Resurfacing Policies in Asphalt Pavement Management to Minimize Costs and Emissions. Journal of Infrastructure Systems, 25, 04019003.

D R Carder, K J Barker, M G Hewitt, D Ritter, A Kiff 2007. Performance of an Interseasonal Heat Transfer Facility for Collection, Storage, and Re-use of Solar Heat from the Road Surface. Published Project Report, PPR 302.

G. Allen Bowers Jr., S. M. ASCE, C. Guney Olgun 2014. Ground-Source Bridge Deck Deicing Systems Using Energy Foundations. Geo-Congress Technical Papers, 234, ASCE 2014.

Gaoyang Hou, Hessam Taherian, Ying Song, Wei Jiang, Diyi Chen 2022. A Systematic Review on Optimal Analysis of Horizontal Heat Exchangers in Ground Source Heat Pump Systems. Renewable and Sustainable Energy Reviews, 154, 111830.

Liang Pu, Lingling Ho, DiQi, Yanzhong Li 2018. Structure Optimization for Horizontal Ground Heat Exchanger. Applied Thermal Engineering, 136, 131-140.

Salsuwanda Selamat, Akio Miyara, Keishi Kariya 2016. Numerical Study of Horizontal Ground Heat Exchangers for Design Optimization. Renewable Energy, 95, 561-573.

Wei Si, Biao Ma, Ning Li, Jun-ping Ren, Hai-nian Wang 2014. Reliability-based Assessment of Deteriorating Performance to Asphalt Pavement under Freeze–thaw Cycles in Cold Regions. Construction and Building Materials, 68, 572-579.

Wenke Zhao, Yaning Zhang, Lei Li, Wentao Su, Bingxi Li, Zhongbin Fu 2020. Snow Melting on the Road Surface Driven by a Geothermal System in the Severely Cold Region of China. Sustainable Energy Technologies and Assessments, 40, 100781.

Xiaoyu Gu, Nikolas Makasis, Yaser Motamedi, Guillermo A.Narsilio, Arul Arulrajah , Suksun Horpibulsuk 2022. Geothermal Pavements: Field Observations, Numerical Modelling and Long-term Performance. Geotechnique, 72, No 9, 832-846.